

Article

Brake Particle PN and PM Emissions of Battery Electric Vehicles (BEVs): On-Vehicle Chassis Dynamometer Measurements

Panayotis Dimopoulos Eggenschwiler *, Daniel Schreiber and Nora Schüller 

Empa, Swiss Federal Laboratories for Materials Science and Technology, Chemical Energy Carriers and Vehicle Systems Laboratory, CH-8600 Dübendorf, Switzerland; daniel.schreiber@bluewin.ch (D.S.); nora.schueller@empa.ch (N.S.)

* Correspondence: panayotis.dimopoulos@empa.ch; Tel.: +41-58-765-4337

Abstract

Currently, brake particle emissions from traffic are considered one of the dominant sources of particulate matter in the atmosphere. A recent question concerns the contribution to brake particles of Battery Electric Vehicles (BEVs). The present work assesses brake particle emissions by measurements of particle number (PN) and mass (PM) of three light-duty BEVs. One front disc brake of each vehicle has been enclosed in a customized casing with appropriate ventilation for forming the aerosol. All three BEVs have been measured on a two-axis chassis dynamometer. The BEV relying more on electric braking (some 68% of the braking energy was covered by electric braking) had the lowest brake PN emissions over the (emissions) WLTC at $6.4 \times 10^9 \text{ km}^{-1}$ per front brake. This was less than half with respect to the other BEV (where only 52% of the braking energy was electric). PM emissions of the two vehicles were similar at 0.93 mg/km for PM < 12 μm and 0.65 mg/km for PM < 2.5 μm , both for one front brake. However, one of the measured BEVs had extraordinarily high PN emissions, some 23 times higher than the lowest-emitting BEV. The difference in PM was not as high, but was some four times higher.

Keywords: brake PN; PM; Battery Electric Vehicles (BEVs); real vehicle use; chassis dynamometer

1. Introduction

Aerosol particles from traffic are a major pollution source in urban environments [1–4]. Particulate emissions from vehicles consist of exhaust particles, generated in the combustion process, and non-exhaust particles, which are either generated by brake and tire wear or already exist on the road surface and are resuspended by the vehicles [5]. All exhaust emissions have drastically reduced in the last 30 years due to regulations, which improved exhaust aftertreatment as well as the electrification of the transportation sector. Currently, non-exhaust emissions are similar to or even higher than exhaust emissions.

Vehicle brakes contribute a significant share of traffic-related particle emissions. Studies report that brake wear particles (BWPs) can account for a share of up to 21% of the total PM₁₀ load emitted by vehicles in urban areas [6,7]. Based on published work (e.g., [8–11]), some 35–55% is airborne, the remainder staying either on the brakes or depositing on the road.

The composition of the emitted BWP is given by the brake material configuration [12,13], the associated friction properties, the operating parameters and the friction partners' temperature [14,15]. Brake pads consist of different materials in generally undisclosed proportions. Studies ascribe Fe, Zn, Cu, Sb, and Ba to the main BWP constituents



Academic Editor: Long Wei

Received: 19 November 2025

Revised: 25 December 2025

Accepted: 30 December 2025

Published: 31 December 2025

Copyright: © 2025 by the authors.

Licensee MDPI, Basel, Switzerland.

This article is an open access article distributed under the terms and conditions of the [Creative Commons Attribution \(CC BY\)](https://creativecommons.org/licenses/by/4.0/) license.

and use those as tracers for identifying and quantifying brake particles in the ambient air [16–18]. The increasing temperature of the friction partners in operation results in evaporation of organic materials from the pads, resulting in hydrocarbon emissions [19,20]. Oxidation of metallic components results in metal oxide emissions [20]. The emitted organic components are the source of abundant particles smaller than 200 nm. Nanoparticles smaller than 40 nm have also been identified [21]. Furthermore, high friction partner temperatures initiate delamination on the brake pad surface, generating particles above 2.5 μm [22].

BWP quantification results are not easily comparable, since they have been obtained with different methods. Reported results are not directly comparable, sometimes even contrasting [23–25]. The different setups used until now include specific brake dynamometers [22,25–28], Pin-on-Disc measurements [29–32], and chassis dynamometer measurements involving an entire vehicle [21,23,33,34]. Furthermore, measurements based on sampling directly in the vicinity of the brakes on the road [26] have also been reported. The most widely used method, the brake dynamometer, is rather simple to use, offering high control possibilities. Chassis dynamometer tests are significantly more complex and time-consuming on the one hand; on the other, though, the results can be considered as closer to real driving emissions.

The standardization of brake particle emission measurements is currently one of the main items of the Working Group on Energy and Pollution (GRPE), a member of the Particle Measurement Program Informal Working Group (PMP-IWG). The main aim is the development of a global technical regulation (UN GTR No. 24) for reproducible quantification of BWP emitted by light-duty vehicles weighing up to 3.5 tons [6,7]. The setup for sampling, as well as for reproducible quantification of BWP [35–41] on a defined brake test bench (without a vehicle), has been the focus. A further point has been the definition of a cycle similar to the worldwide harmonized certification cycle for light-duty vehicles (WLTC) on a brake test bench [36–38], under the name WLTP-Brake. Results of international, interlaboratory comparable measurements (also on an identical vehicle with identical brake components) have been published recently [39–41]. The WLTP-Brake should not be confused with the WLTC cycle for determining vehicle exhaust emissions. While the WLTP-Brake cycle involves the brakes on a specific dynamometer (without the vehicle), for the WLTC emission cycle, the entire vehicle is on a chassis dynamometer, which has to be adjusted in order to reproduce the vehicle's resistance characteristics.

The present work has the goal of contributing to the assessment of the BWP of Battery Electric Vehicles (BEVs). BEVs are heavier than their combustion engine counterparts because of the weight of the battery. Therefore, increased BWP emission can be expected. On the other hand, BEVs use the possibility of electric braking, recuperating energy in the battery, thus reducing mechanical braking and associated BWP emissions. Each braking event involves both types of braking [42]. Vehicle manufacturers rely on different distributions of the braking energy in the two braking modes based on their own criteria for safe, reliable and comfortable vehicle decelerations. The distribution of the braking energy in electric and mechanical braking is also crucial for evaluating the measurements on a brake dynamometer for a BEV. Currently, there is an open discussion concerning this distribution. More electric braking results in lower brake particle emissions; this is clear. This distribution is also taken into account in extrapolating the results on a brake dynamometer for obtaining the total brake particle vehicle emission.

Furthermore, vehicle manufacturers offer BEV drivers the option to choose among different vehicle modes, resulting in more sporty, comfortable and/or ecological vehicle behaviour. The present work addresses the question of whether these different vehicle modes affect the brake particle emissions. In addition, the effect of the battery State of

Charge, SoC, on the BWP emissions is investigated. A fully charged battery does not permit any electric braking. A distance travelled with a fully charged battery may result in higher BWP emissions with respect to starting it with a lower-charged battery. In parallel, battery depletion is fast, resulting in the availability of electric braking. To our knowledge so far, there have not been any reports of brake particle emissions of BEVs measured on a chassis dynamometer, considering the different vehicle parameters mentioned above.

Therefore, three BEVs from different manufacturers have been equipped with specifically designed and realized parts (presented in detail in [21]) for extensive measurements of the BWP emissions on the chassis dynamometer. The measurements allowed direct comparisons with a similar ICE and a hybrid electric vehicle measured with similar equipment in the identical chassis dynamometer.

2. Experimental Setup

2.1. PN and PM Measurement Setup

The measurement setup was designed and realized in close accordance with the Particle Measurement Program (PMP) protocol for the quantification of exhaust particles. Figure 1 shows the vehicle, as well as the instrumentation setup used for measuring brake PN and PM emissions of light-duty Battery Electric Vehicles (BEVs) on the chassis dynamometer in the present work. The identical setup was used for PN and PM measurements of a gasoline, as well as of a hybrid electric vehicle [21].

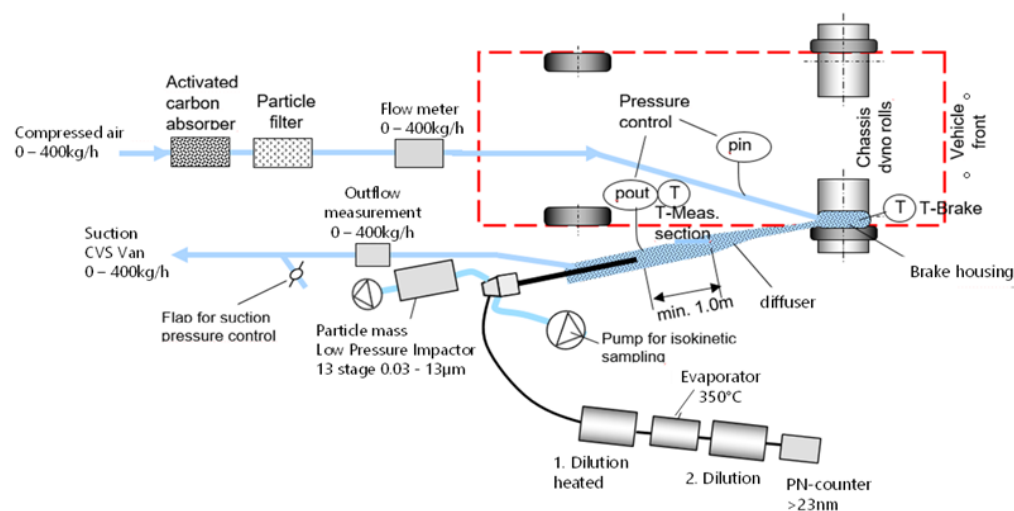


Figure 1. Experimental setup on the chassis dynamometer with the instrumentation for measuring brake particles.

For the aerosol necessary for carrying the brake particles, an ambient air compressor with integrated drying was used. The air was adequately filtered, so that the brake housing was supplied with clean and sufficient scavenging airflow of 220 kg/h. The scavenging air flow was chosen such that the temperatures on the right (in the housing) and the left (not modified) front brake of the vehicle were almost equal. Downstream the brake, the aerosol was discharged with a suction blower in order to achieve a slight overpressure in the brake housing towards the instruments for the assessment of particle number (PN) and particle mass (PM). The measurement setup is shown with some further details in Figure 2. Further details of the instruments used can be found in [21].

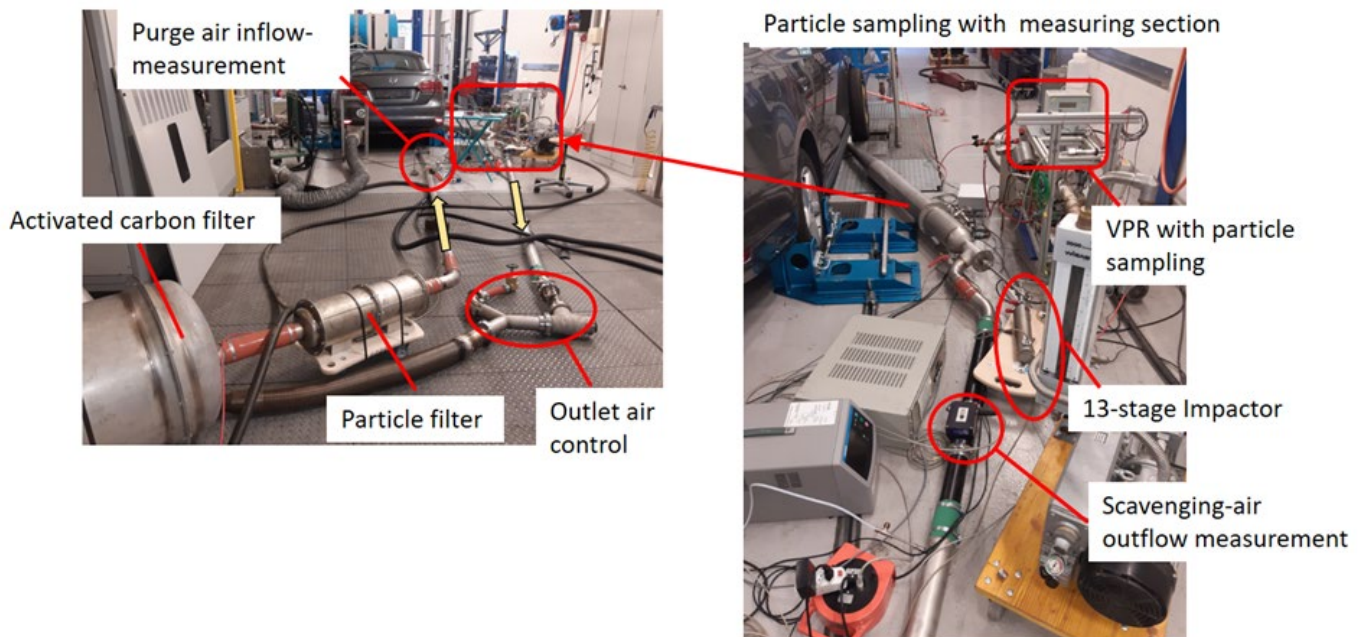


Figure 2. Details of the experimental setup for the measurement of brake PN and PM emissions on the chassis dynamometer (corresponding with the technical schematic of Figure 1).

2.2. Vehicle Modifications

The front right brake disc was enclosed in an in-house designed and manufactured casing with a rolling mechanical seal. The space necessary for the brake housing in and partly out of the wheel arches was gained by an extension added to the front axle, so the distance between the two front wheels was slightly increased with respect to the on-road vehicle. The brake housing (the lower half of it) is shown in Figure 3a. In the centre, the extension can also be seen. The vehicle's emergency wheel was mounted on the extender. In Figure 3b, the enclosed brake is behind the emergency wheel. The outflow pipe can also be seen in the lower left corner. This assembly was chosen in order to have minimal changes to the vehicle geometry and accommodate the additional components for the measurements. All parts required precision manufacturing for a good fit in each vehicle.

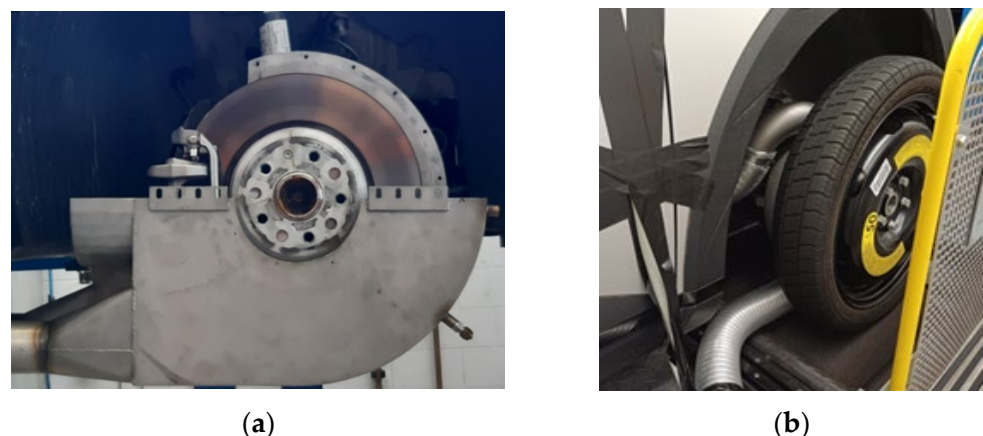


Figure 3. (a) Brake housing (only the lower half for the measurements, and the second half of the housing was also mounted) and (b) measurement configuration with the emergency wheel (and the entire housing and extender behind the emergency wheel).

The emergency wheels have a smaller diameter with respect to the original wheels. Thus, for identical vehicle velocities, the emergency wheel and thus also the brakes have

approx. 25% higher rotation. The brake particles with this assembly may be higher than with the normal wheel. However, the diameter of the emergency wheel used is roughly 10% smaller than the smallest tire diameter approved for the measured vehicles.

The forces on the chassis dynamometer have been measured with the original wheels as well as with the emergency wheels with the brake housing without any noticeable differences. Deceleration forces and energy are identical regardless of the wheels used. This was the fact for all three measured vehicles; thus, the measured results are directly comparable. The brake particle emissions with the original wheels are expected to be slightly lower.

In order to avoid complications with the brake housing in combination with the emergency wheel, the last, extra high velocity (EH) part of the WLTC cycle was not part of all measurements. All measurements of the different vehicles, as well as of the different conditions of each vehicle, consisted of five repetitions of the WLTC cycle without the last, extra high-velocity part, followed by two repetitions of the entire WLTC cycle (with the extra high velocity part). Comparisons in the Results Section are always either without or with the EH part. Reported emission factors use the results of measurements, including the EH part.

A series of specific measurements has been performed to evaluate the experimental setup. The main aims have been as follows:

- Assessment of the influence of the background particle concentrations;
- Determination of optimal scavenging flow;
- Assessment of particle transport efficiencies of the entire setup;
- Monitoring of the brake discs' temperature (at the end of each cycle), assuring that no significant temperature differences are present between the right, front, measured disc (enclosed in the housing) and the left disc (in the regular vehicle configuration).

2.3. Measured Battery Electric Vehicles (BEVs)

In this study, three medium-sized BEVs, typical for the European market of mid-sized light-duty vehicles, have been chosen. The main characteristics of the vehicles related to braking are summarized in Table 1, where we also include the characteristics of an ICE and a hybrid electric vehicle used for the comparisons in Section 3.5. Further details of the ICE and hybrid vehicle regarding brake particle emissions are in [21].

Table 1. Technical characteristics of the measured vehicles.

	BEV1	BEV2	BEV3	ICE	Hybrid
Front brake	Discs	Discs	Discs	Discs	Discs
Rear brake	Drums	Discs	Discs	Discs	Discs
Propulsion	Rear wheel	Four wheel	Rear wheel	Front wheel	Front wheel
Curb weight [kg]	1815	1899	2275	1820	1805
Model Year	2021	2023	2023	2015	2013

While the propulsion configuration should not be of any significance for the conventional (ICE and hybrid) vehicles regarding the brake particle emissions, it may be important for the BEVs, given that only the wheels connected to an electric motor can be used for electric (recuperation) braking.

The vehicles used in this study had serial production friction partners (discs and brake pads). The vehicles have been borrowed from their owners for the measurements, so the friction partners have been used in everyday, regular driving prior to the measurements.

Starting the measurement cycle with a fully charged battery (SoC = 100%) may result in higher brake particle emissions, given the reduced electrical recuperation potential, at least in the early parts of the cycle. Therefore, all cycles have been measured starting with two different SoCs, 100% and 65%.

In general, BEVs offer their users several operating modes to choose from. Apart from the “normal” operation mode, there is the possibility to select a more aggressive, “sporty mode”, a mode for severe weather (snow, etc.), as well as an operation mode focusing on “comfortable driving” relying, among other features, on a more balanced distribution between electrical and mechanical braking. In the present work, we label the comfort-oriented operation mode as “low recuperation” mode. The specific objectives and goals of the vehicle manufacturers behind these operational modes are not known to us and, most probably, differ from manufacturer to manufacturer, as the labelling of these modes also differs. In the present work, the BEVs have been measured in the “normal” operation mode as well as in the “low recuperation” mode, where we expect more mechanical braking and thus also higher brake particle emissions.

2.4. Test Cycle

For the measurements, the current WLTC emission certification cycle for light-duty vehicles was chosen. The emission WLTC driving cycle consists of four parts: low, medium, high, and extra high velocity. The respective maximum velocities (v_{\max}) of each sub-cycle are as follows: low: $v_{\max} \leq 60$ km/h; medium: $60 \text{ km/h} < v_{\max} \leq 80$ km/h; high: $80 \text{ km/h} < v_{\max} \leq 110$ km/h; and extra high: $v_{\max} > 110$ km/h. The time–velocity profile of the cycle can be seen in Figure 4 and Figure 7 in the following section.

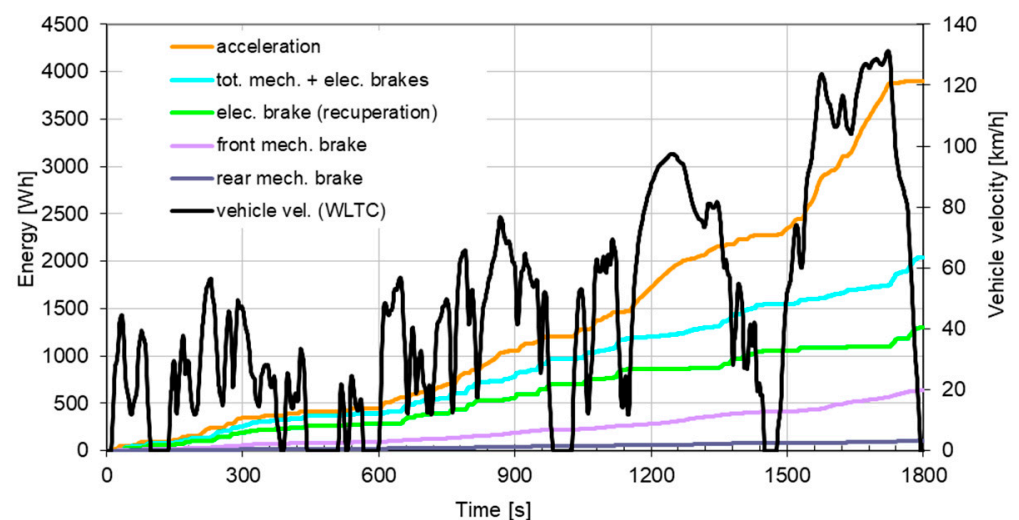


Figure 4. Comparison of the time histories of the different brake energies of BEV3, at normal operation mode and 100% SoC at the test cycle start.

3. Results and Discussion

3.1. Brake Energy Distribution Patterns of the Measured Battery Electric Vehicles (BEVs)

All experiments have been performed on a two-axis chassis dynamometer, enabling the measurement of the energy flow on both vehicle axes during acceleration as well as braking over the WLTC cycle. The time histories of these energy flows are shown in Figure 4, as measured for the BEV3. For this measurement, BEV3 was operated in normal mode while the cycle was started with a fully charged battery (100% SoC). The biggest part of the braking energy is achieved by the electric brake, recuperating energy to the battery (green line). Significantly lower is the braking energy achieved by the mechanical

brakes on the front wheels (light purple line), while the lowest braking energy accounts for the mechanical brakes on the rear wheels (dark purple line). The sum of the total braking energy is shown by the light blue line. As expected, it is clearly lower than the acceleration energy (yellow line).

As seen in Figure 4, some two two-thirds of the braking energy is covered by the electric brake, about one-third thereof by the front wheel mechanical brakes, while a very small fraction is covered by the mechanical rear wheel brakes. This distribution of the brake energy is shown in detail in Figure 5 for five repetitions. Moreover, the results are shown separately for the four parts of the WLTC cycle. The results are almost identical for the five repetitions, while the tendencies are very similar for all parts of the cycle.

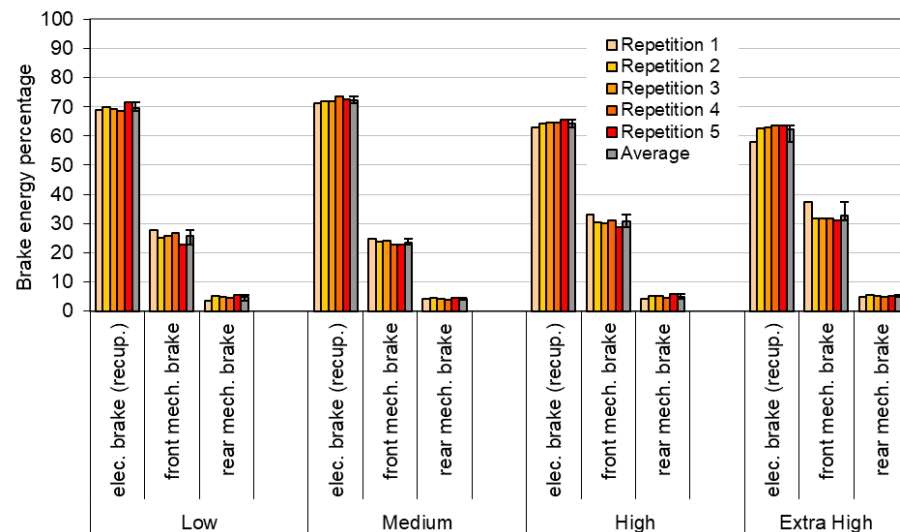


Figure 5. Comparison of the brake energy distribution in electric and mechanical brakes (front and rear axle) of BEV3, at normal operation mode and 100% SoC at the test cycle start (5 repetitions at identical starting conditions).

There is some evidence in Figure 5 that in the last two WLTC parts with the highest vehicle velocities, the mechanical brakes are used more than in the first two parts with the lower velocities. It is likely that in the two highest velocity parts of the cycle, the necessary braking power sometimes exceeds the maximal battery charging power, resulting in more mechanical braking. The other two measured BEVs had more mechanical braking in the last two parts of the WLTC cycle and less in the first two parts.

The general pattern for BEV3 is evident: Some 68% of the braking energy is electrical, recuperating energy to the battery. Some 27% of the braking is mechanical by the front axis, while the remaining 5% (also mechanical) is by the rear axis brakes. This pattern differed significantly for the three measured BEVs (Table 2). The electric brakes have been used for only 52% of the braking energy by BEV1, while BEV2 had 54% of the total brake energy covered by electrical braking.

Table 2. Brake energy distribution of the 3 measured BEVs over the WLTC cycle.

	BEV1	BEV2	BEV3
Electric brake (recup.)	52%	54%	68%
Front mech. brake	33%	36%	27%
Rear mech. brake	15%	10%	5%

Figure 6 shows the brake energy distribution of BEV3 when starting the WLTC at two different State of Charges (SoCs) of the battery, as well as at normal driving mode and the reduced recuperation driving mode. It is evident that the differences are very small. Starting with a not fully charged battery (SoC = 65%) allows slightly more recuperation at the beginning of the cycle. As soon as some of the battery charge is depleted, recuperation is fully available, so that over the entire WLTC cycle, differences are small, however discernible and plausible. The measurements with SoC = 65% at cycle beginning used electric braking slightly more than those with SoC = 100% (and mechanical braking slightly less). Please note that in Figure 6, most of the WLTC repetitions did not include the extra high (EH) part. As can be seen, this affected the brake energy distribution by only a few percentages. The “low recuperation” driving mode resulted in slightly higher electric braking use.

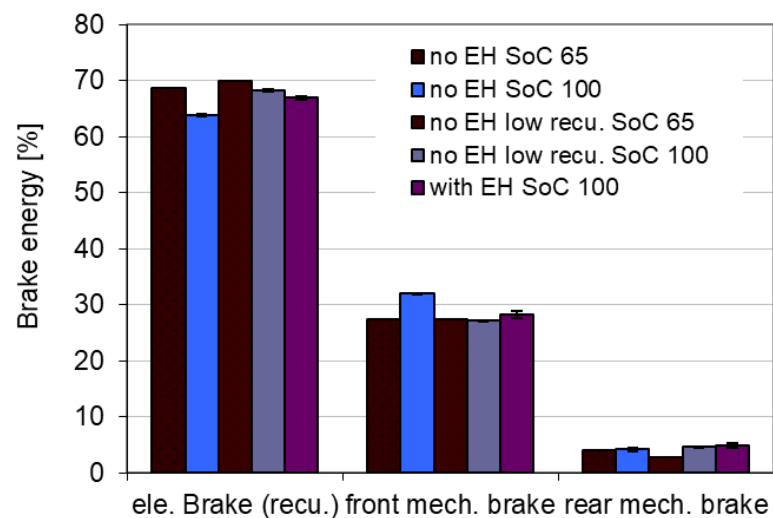


Figure 6. Brake energy distribution of BEV3 at different vehicle parameter configurations.

In summary, the different driving modes, as well as the different SoCs at the start of the cycle, do not affect the brake energy distribution among electrical and mechanical braking much. This was similar for BEV1 and BEV2.

3.2. Brake Particle Number (PN) Emissions

The brake PN emission concentrations of BEV3 during five consecutive WLTC cycles are shown in Figure 7; brake particles (PN) are released in discrete events with peaks of differing heights. In each repetition, the emission events occur in almost identical time instants; however, the emitted quantities differ. Mainly, two reasons have been identified leading to these PN emission peaks; some of these peaks are clearly associated with braking (decelerations), as can be seen in Figure 8 (framed in blue).

Some other peaks appear during accelerations (phases with no braking), after the vehicle exceeds higher velocities (>60 km/h) (Figure 8 framed in red), clearly not associated with braking. These correspond to emissions of brake particles produced in earlier braking events that remained on the friction partners. With increasing vehicle velocity, the increasing aerodynamic forces drag these deposited particles off the friction partners. This emission characteristic was very similar for all three measured BEVs, as well as for a hybrid and a conventional ICE light-duty vehicle we have measured [21]. However, the emission quantities differ strongly.

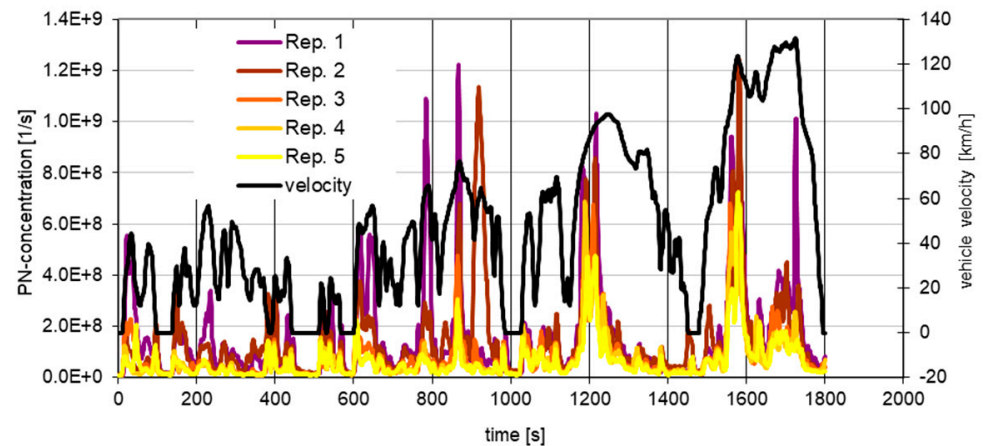


Figure 7. PN emissions of BEV3 during 5 consecutive WLTC cycles (normal operation mode with 100% SoC of the battery at the beginning of the cycle).

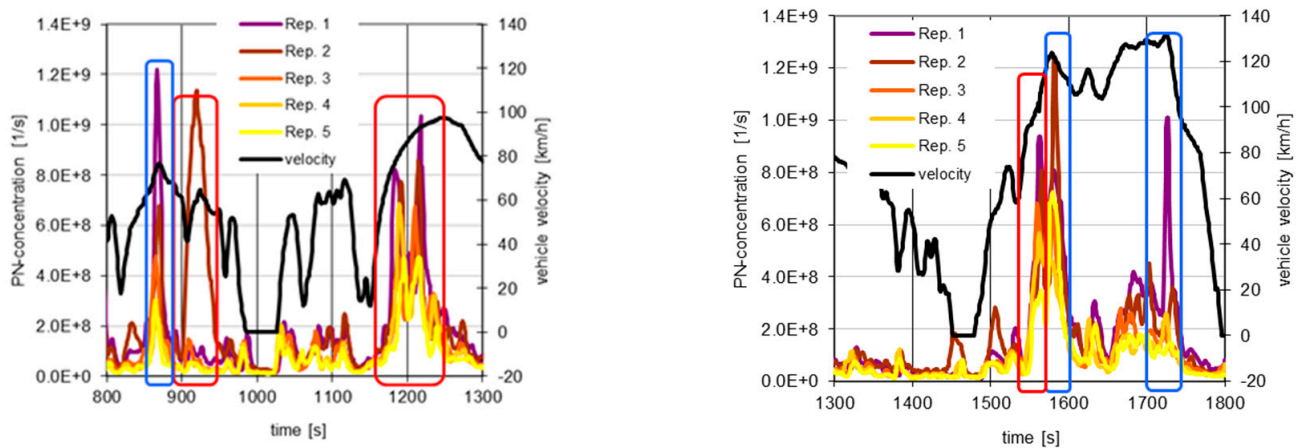


Figure 8. PN emissions of BEV3 during 5 consecutive WLTC cycles, with excerpts from Figure 7 highlighting peaks caused by braking (blue frames) and by aerodynamic drag (red frames), stripping brake particles off the friction partners at high vehicle velocities (red frames), (all normal operation mode with 100% SoC of the battery at the beginning of the cycle).

Almost all discrete emission events occur at identical instants in all five repetitions. With each repetition though, PN emission quantities decrease (lower peaks at each consecutive repetition) by more than a factor of two; however, after the third repetition, the PN emissions stabilize. This effect has been observed and described in recent publications [21,38–40], as the so-called “bedding effect”. Wear particles from the pad and disc aggregate to form a friction film mainly on the pad surface but also on the disc. This film breaks down from time to time, in particular during brake events with high forces. Thus, the brake particle emissions are strongly dependent on the history of the friction partners. This “bedding effect” is described but poorly understood, and no reliable quantifications exist, since it strongly differs from vehicle to vehicle. The current best practice advice is prescribing 5 cycle repetitions while using only the last two cycles for obtaining reliable PN emission results [40]. Characteristics of the bedding effect at the different measurements of BEV3 are in the Supplementary Material. The measurement series of BEV3 showed a very similar “bedding behavior” with BEV2. The “bedding effect” of PN measured with both BEVs was also very similar to measurements of conventional ICE/hybrid vehicles [21]. In contrast, BEV1 did not show similar “bedding behavior”. The brake PN emissions of BEV1 increased with each repetition, with only a modest tendency towards stabilization after the fifth repetition (thus, having rather an inverse bedding effect). As can be seen in

Section 3.4, BEV1 had exceptionally high brake PN emissions. The results presented in Sections 3.4 and 3.5 evidence that the brake particles of BEV1 are smaller with respect to those of BEVs 2 and 3. These allude to a high-emitting material combination of the pads and/or the disc.

3.3. Brake Particle Mass (PM) Emissions

The absolute accumulated particle concentrations (mg/Nm^3) on each foil (Stage 1–12) of the impactor are shown in Figure 9, clearly evidencing that the overall brake PM emission and, therefore, even more pronounced in each size class, is very low, however significantly higher than the background. The particles with an aerodynamic diameter of roughly $0.309\text{--}7.88\ \mu\text{m}$ account for the most brake wear PM. Ultrafine particles are also clearly present. In our previous work [13], we have examined the morphology of brake particles. The ultrafine particles are rather spherical, and we expressed the hypothesis that they are a result of high temperatures of the friction partners, leading to evaporation and recondensation of, at least a part, of the brake wear matter. As expected, the highest PM emissions have been measured on the WLTC cycles, including the extra high (EH) velocities' part. Interestingly, the "low recuperation" mode resulted in almost all size classes in much higher PM emissions (for almost an order of magnitude) than the normal mode. That this difference was not as high for the PN emissions, evidences that in "low recuperation" mode brake particles are of large size (i.e., more mechanical braking at lower temperatures of the friction partners). Currently, there is strong scientific evidence that particulate emissions are related to the brake disc temperature [15,43].

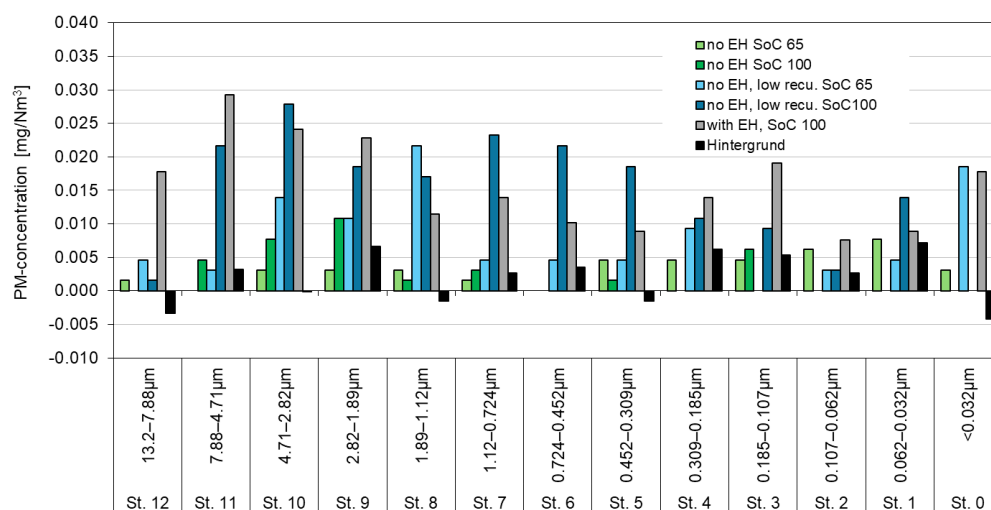


Figure 9. PM concentrations of BEV3 over WLTC cycles starting with a different State of Charge (SoC) of the battery, at two different operating modes, as well as with and without the extra high (EH) velocity component of the WLTC cycle.

Interestingly, Figure 9 shows a clear shift in the modal distribution among the cycles with the lowest friction partners temperatures (low EH, low recu. SoC 100) and the one with the highest (with EH, SoC 100). While both are rather bimodal, the former has one mode at approx. $4\ \mu\text{m}$ and one at $0.6\ \mu\text{m}$, the latter one at $6\ \mu\text{m}$ and one at $0.2\ \mu\text{m}$. Mass size distributions are expected to be unimodal with the typical modes around $1\ \mu\text{m}$ and $6\ \mu\text{m}$ [7,12,14]. In contrast, e.g., in [43] bi- or even multimodal particle number size distributions are reported with at least one peak in the fine and/or ultrafine fraction and an increased share of particle mass in the PM_{2.5} range.

The brake PM emissions of BEV1 have been significantly higher, some four times more. The corresponding PM emissions of BEV2 were like those of BEV3; BEV2 had more in the

bigger size classes and less in the smaller. However, BEV1 and BEV2 had rather unimodal size distributions with the peak being at 4 μm and 2 μm , respectively.

3.4. Brake Particle Morphology (SEM Imaging)

The morphology of the brake particles differed significantly among the vehicles. Bigger brake particles from BEV1 were rather uniformly shaped (Figure 10A,B). Smaller particles of BEV1 have less regular shapes and are inhomogeneous (Figure 10C,D). In contrast, the bigger brake particles of BEV3 (Figure 10E,F) are very irregular, indicating a mechanical abrasion origin. Smaller brake particles of BEV3 have more regular shapes and appear to be homogeneous. For both vehicles, there are abundant brake particles around 100–400 nm.

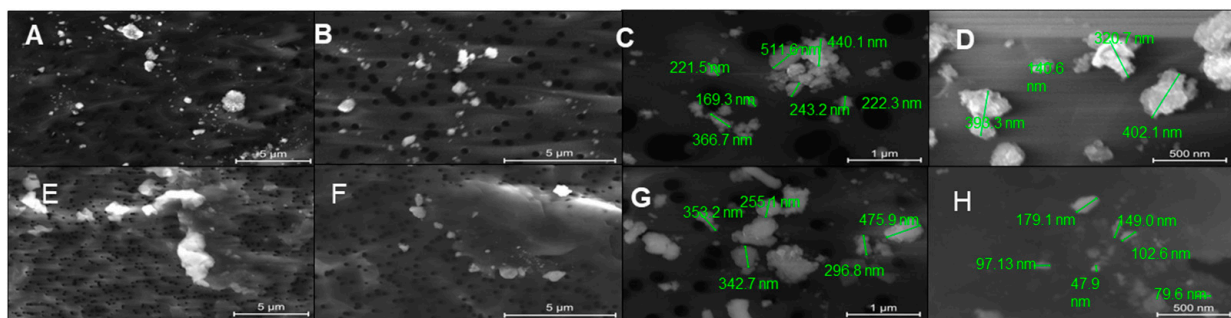


Figure 10. SEM images of BEV1 (A–D) and BEV3 (E–H) at 20,000 \times , 30,000 \times , 100,000 \times and 200,000 \times magnifications.

3.5. Brake Particle PN and PM Emission Factors

In Figure 11, the average brake PN emissions of BEV3 are shown in [PN/km] corresponding to the measurements as of Figure 9. As an overall average, a rough value of 7×10^9 1/km can be kept in mind. Starting the cycle with a fully charged battery, 100% SoC, results in slightly higher emissions than with 65% SoC. Furthermore, the low recuperation mode has clearly higher PN emissions with respect to the normal mode. On the other hand, the higher PN emissions in the cycles with the extra high (EH) part (see Figure 9) do not lead to higher emission factors, given that with the extra high part, the distance (kilometres) increases disproportionately. This decrease in the PN emissions, when including the EH WLTC cycle part, was not the case for all three examined BEVs; including the PN emissions during the EH cycle part resulted in an increase in PN for BEV2. Recently, an interlaboratory study on ICE light-duty vehicles involving 16 participating labs and with five brake systems, with measurements on a brake dynamometer, reported concentrations of 9.4×10^8 – 1.1×10^{10} 1/km/brake [40]. So, BEV3 in this study, with an average of 7×10^9 1/km/brake, lies somewhere in the lower quartile. Reference [15] reports average brake PN emissions of 4.9×10^{10} 1/km/brake. Both [15,40] used the WLTP-Brake cycle on a brake dynamometer. On the other hand, [44] reports values 4.1×10^7 – 1.7×10^9 1/km/brake measured directly on a school bus in real-world driving conditions.

Figure 12 shows the measured brake PN emissions for all three measured BEVs in comparison to a similarly sized conventional ICE vehicle as well as to a hybrid vehicle. All five vehicles have been measured under very similar conditions on a chassis dynamometer as described in Sections 2.1 and 2.2, and with the exhaust emission certification WLTC. BEV2 and BEV3 demonstrate the potential for reducing brake particle emissions with BEVs. The brake PN emissions of BEV3 are nine times lower with respect to those of the ICE and the hybrid vehicle. The brake PN emissions of BEV2 are almost three times lower. BEV1, though, had significantly higher brake PN emissions.

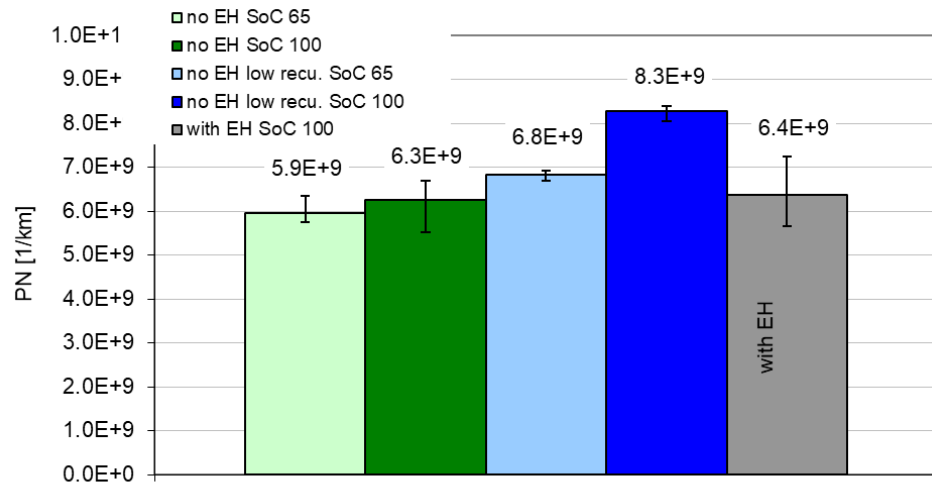


Figure 11. Average brake PN emission in [PN/km] of BEV3, starting the cycles with different State of Charges (SoCs) of the battery, at two different operating modes (normal, not labelled, and low recuperation) as well as without or with the extra high (EH) velocity part of the WLTC cycle, from the measurements on one front disc brake (for each bar, 5 WLTC repetitions have been measured, and the average is taken over the 3 last repetitions).

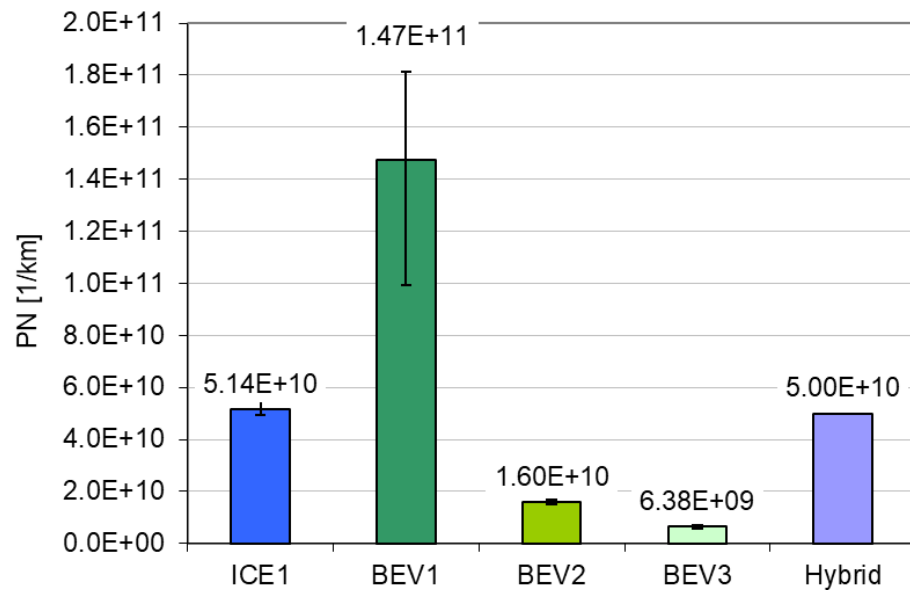


Figure 12. Average brake PN emissions of the measured three BEVs: one conventional ICE, and a hybrid vehicle of comparable size, measured on one front disc brake. The results shown are derived from the entire WLTC cycle (including the extra high velocities' part). BEVs and the hybrid vehicle with 100% SoC at the cycle start, all vehicles operated at normal mode.

This result is of particular interest, taking into account that BEV3 is the heaviest of all measured vehicles (see Table 1). It demonstrates the potential in reducing brake particle emissions with an appropriate layout of the brakes and the braking process.

These measurement results can be used for total PN emission factor estimations. It is important to keep in mind that the measurements and the results shown in Figures 11 and 12 have been performed on one of the front brakes. The numbers must be doubled to obtain the emissions of both front wheels and brakes.

For BEV1, the total emission factor is given by the value in Figure 12 multiplied by a factor of two, taking into account the rear drum brakes of the vehicle and assuming that no brake particle emission can escape from those. Measurements of the brake particle

emissions of drum brakes exist [39,40] on brake dynamometers. Drum brakes emit much lower particles due to their enclosed nature; however, they are not zero. Our experimental setup can be adapted for drum brakes, but with significant effort. We are not aware of any measurements on vehicles on the chassis dynamometer. However, the brake particle emissions of BEV1 are already very high; adding the contribution of the rear drum brakes will not change the overall picture.

For BEV2 and BEV3, the values of Figure 12 are doubled to account for the emissions from the second front brake, while the factors for approximating the contribution of the rear axis brakes in the total PN emissions are taken based on the brake energy distribution as measured and reported in Figures 5 and 6 and Table 2. A similar procedure was followed for ICE1 and the hybrid vehicle.

The (PM) from a single WLTC cycle, given by the sum of the 13 stages of the impactor (13 differential measurements), showed rather high variability, given the quite low values from each individual measurement. Therefore, the cycles have been repeated three times, leaving the foils in the impactor. Thus, the used loadings for the values reported below are averaged over three consecutive WLTC cycles. The determined emission factors, shown in Figure 13, result in an average value of some 0.5 mg/km for PM < 12 μm and 0.4 mg/km for PM < 2.5 μm . The measurements, including the extra high part, result in higher values. The impact of the battery State of Charge (SoC) in normal operation is not clear; the measured values are, anyhow, very low. The “low recuperation” mode, on the other hand, leads clearly to higher PM emissions. In this mode, starting the cycle with 100% SoC of the battery results in higher PM emissions. Interestingly, the tendencies in Figure 11 are very similar to those in Figure 13.

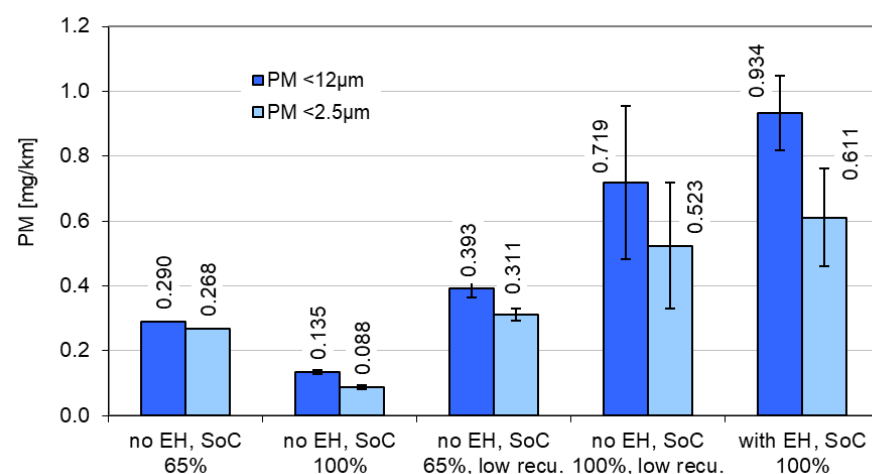


Figure 13. Average brake PM emission in [mg/km] of BEV3 starting the cycles with different State of Charge (SoC) of the battery, at two different operating modes (normal, not labelled, and low recuperation) as well as without or with the extra high (EH) velocities part of the WLTC cycle, as from the measurements on one front disc brake.

Figure 14 shows the measured brake PM emission of the three BEVs in comparison to the similarly sized conventional ICE and hybrid vehicles. PM emissions of BEV2 and BEV3 are about a third of those of the ICE and the BEV1 vehicle. The PM emissions of hybrid vehicles were closer to those of the ICE and BEV1. Interestingly, the PM emissions of BEV2 are similar to those of BEV3. Since the PN emissions of BEV2 were more than double as high as the corresponding ones of BEV3 (see Figure 12 and Table 3), it can be inferred that the brake particles emitted by BEV2 are significantly smaller (and thus have with higher environmental and health impact).

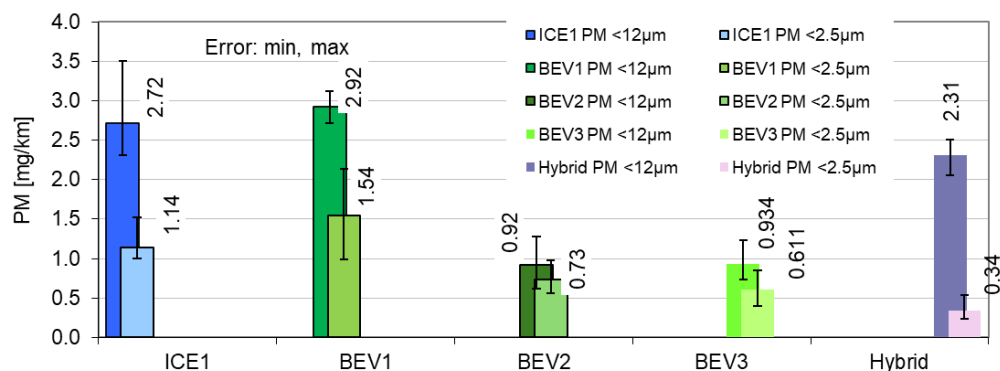


Figure 14. Brake PM emissions of the measured two BEVs and one conventional ICE vehicle of comparable dimensions, as measured with the identical equipment on one front disc brake. The shown results are derived from the entire WLTC cycles (including the extra high velocities’ part). BEVs with 100% SoC at the cycle beginning, all vehicles operated at normal mode.

Table 3. Estimated total brake PN emission factors over the WLTC cycle based on the measurement results shown in Figure 12 and assuming that the second front brake has identical emissions, while approximating the rear brake emissions based on the front–rear brake energy distribution.

	ICE	BEV1	BEV2	BEV3	Hybrid
Total brake PN [1/km]	1.54×10^{11}	3.0×10^{11}	3.37×10^{10}	1.31×10^{10}	1.5×10^{11}

The measured and shown values in Figure 14 are in the lower area of the reported values. The measurements summarized in [39] conclude in PM2.5 and PM10 emissions that varied between 0.8 and 4.0 mg/km and 2.2–9.5 mg/km per brake, respectively, depending on the type of brake and the applied testing load. The test matrix covered a wide variety of brake systems and configurations. Almost 37–45% of the emitted PM falls in the fine particle size, with this fraction being higher for the drum brake. On the other hand, almost 50–65% of the total brake mass loss falls in particle sizes larger than 10 µm or escapes quantification [39]. In a very similar order of magnitude are the PM emissions reported in [15]. PM10 of 4.6 mg/km per wheel for an ICE vehicle is the conclusion. Ref. [45], on the other hand, provides distinctive results for two different types of braking pads, low-steel and non-steel pads. The former resulted in a PM10 emission of 3.9 mg/km per brake (per 1000 kg of vehicle mass); however, it had quite a high variability in the results. The latter had a PM10 emission of 0.4 mg/km per brake.

Based on the measurements in the present work and with the results on the brake PM emissions on one of the front wheels, as shown in Figure 14, the PM emissions factors have been derived. The approach, therefore, has been described in the PN-related discussion. The PM emission factors are shown in Table 4.

Table 4. Estimated total brake PM emission factors over the WLTC cycle based on the measurement results shown in Figure 14 and assuming that the second front brake has identical emissions, while approximating the rear brake emissions based on the front–rear brake energy distribution.

	ICE	BEV1	BEV2	BEV3	Hybrid
Total brake PM < 12 µm [mg/km]	8.16	5.84	1.91	1.93	6.93
Total brake PM < 2.5 µm [mg/km]	3.42	3.08	1.25	1.53	1.02

4. Conclusions

Measurements of the brake particle PN and PM emissions have been performed on three Battery Electric Vehicles (BEVs) on the chassis dynamometer. Therefore, one of the front brakes of each vehicle has been enclosed in a custom-designed housing with controlled ventilation. In parallel, the brake energy distribution among electric braking (recuperation of electric energy in the battery) and mechanical braking in the front and rear vehicle axes could be determined.

The three measured BEVs use the possibility of electric braking to different degrees. The measurements show that BEV3 used electric brakes for some 68% of the braking energy during the WLTC cycle. The other two BEVs measured used electric braking to a lesser extent, around 50%. The largest part of the mechanical braking energy is accrued at the front axis (>25% of the total braking energy), while the smallest part is at the rear axis (>5%). Different State of Charges (SoCs) of the battery at the beginning of the cycle, as well as different driving modes (selectable by the vehicle's users), had only a minor influence on the distribution of the brake energy.

Brake particle PN emission characteristics showed a very similar pattern for all vehicles measured. Brake PN emissions occur at discrete events, associated either with

- Braking events;
- Higher vehicle velocities (>60 km/h), where aerodynamic forces strip brake PN off the friction partners.

BEV3, the one relying more strongly on electric braking, had the lowest brake PN emissions, less than half in respect to BEV2. PM emissions of the two vehicles were similar. This shows that BEV2 emitted more small particles than BEV3. BEV3 had more than eightfold lower PN emissions with respect to the ICE and the hybrid vehicles. However, BEV1 had extraordinarily high PN emissions, some 23 times higher than BEV3. The difference in PM was not as high; BEV1 emitted four times more PM than BEV3 (also evidencing that BEV1 emitted more small particles).

Based on the measurements performed on a single front wheel, total emission factors (for the entire vehicle) have been estimated. The results show the following:

- Total brake PN emission factors of the two low PN-emission BEVs are in the order of 2×10^{10} [1/km], thus being slightly lower, or similar to the exhaust PN of conventional ICE vehicles equipped with the latest aftertreatment technologies.
- Total brake PN of the two low PN-emission BEVs is some five times lower than that of a conventional ICE and a hybrid vehicle of comparable size.
- The third measured BEV had, in contrast, high brake PN emissions, an order of magnitude higher than the other two measured BEVs, twice as high as the ICE and the hybrid vehicle.
- Total brake PM emission factors of the two low-emission BEVs are in the order of 2.0 mg/km for particles smaller than 12 μm and 1.4 mg/km for particles smaller than 2.5 μm .
- The total brake PM of the two low-emission BEVs is roughly two times lower than that of a conventional ICE.
- The third measured BEV had, in contrast, high brake PM emissions, almost an order of magnitude higher than the other two measured BEVs, and three times as high as the ICE.

The results demonstrate the potential of electric braking in reducing brake particle emissions. The brake particle emissions of BEV3 are very low. Regulation should take into account the effective portion of the electric braking of the vehicles in question. On the other hand, the high-emitting BEV1 demonstrates clearly that regulatory limits are necessary in

order to enhance efforts for the development of low-emission brake systems in combination with the vehicles these are used in.

Supplementary Materials: The following supporting information can be downloaded at: <https://www.mdpi.com/article/10.3390/atmos17010059/s1>, Figure S1. Total PN emissions of BEV3 at 5 consecutive WLTC cycles, (normal operation mode with 100% SoC of the battery at the beginning of the cycle), Figure S2. PN emissions of BEV3 at 5 consecutive WLTC cycles starting the cycles with different State of Charge (SoC) of the battery, at two different operating modes (normal, not labelled, and low recuperation) as well as without or with the Extra High (EH) velocities part of the WLTC cycle.

Author Contributions: Conceptualization, P.D.E. and D.S.; methodology, P.D.E. and D.S.; software, D.S.; validation, P.D.E., D.S. and N.S.; formal analysis, P.D.E. and D.S.; investigation, N.S. and D.S.; resources, D.S.; data curation, D.S.; writing—original draft preparation, P.D.E.; writing—review and editing, P.D.E., D.S. and N.S.; visualization, P.D.E. and D.S.; supervision, P.D.E. and D.S.; project administration, P.D.E.; funding acquisition, P.D.E. All authors have read and agreed to the published version of the manuscript.

Funding: The present work was carried out within the framework of a project funded by the Swiss Federal Office of Environment (BAFU), contract number 19.0106.PJ/B92FC56C1. The authors express their gratitude.

Institutional Review Board Statement: Not applicable.

Informed Consent Statement: Not applicable.

Data Availability Statement: All data presented in this study are available on request from the corresponding author. The data are not publicly available due to confidentiality agreements with the part providers.

Conflicts of Interest: The authors declare no conflicts of interest. The funders had no role in the design of the study; in the collection, analyses, or interpretation of data; in the writing of the manuscript, or in the decision to publish the results.

Abbreviations

The following abbreviations are used in this manuscript:

BEV	Battery electric vehicle (light-duty).
BWPs	Brake wear particles.
EHs	Extra high velocities—part of the WLTC cycle.
ICE	Internal combustion engine-powered vehicle (light-duty).
Low recu.	Vehicle use mode (selectable by the driver) for more comfortable vehicle behaviour.
PM	Particle mass.
PMXX	Mass of particles with a diameter below XX μm , i.e., PM2.5 gives the mass of all particles with a diameter below 2.5 μm .
PMP	Particle Measurement Program, established by UNECE (=United Nations Economic Commission for Europe).
PN	Particle number.
Rep.	Indication of the repetition of a measurement under identical conditions.
SEM	Scanning electron microscope.
SoC	State of charge of the propulsion main battery of a BEV.

References

1. Meister, K.; Johansson, C.; Forsberg, B. Estimated Short-Term Effects of Coarse Particles on Daily Mortality in Stockholm, Sweden. *Environ. Health Perspect.* **2012**, *120*, 431–436. [[CrossRef](#)]
2. Pope, C.A.; Dockery, D.W. Health Effects of Fine Particulate Air Pollution: Lines That Connect. *J. Air Waste Manag. Assoc.* **2006**, *56*, 709–742. [[CrossRef](#)]

3. Jiang, R.; Liu, Y.; Hu, D.; Zhu, L. Exhaust and Non-Exhaust Airborne Particles from Diesel and Electric Buses in Xi'an: A Comparative Analysis. *Chemosphere* **2022**, *306*, 135523. [[CrossRef](#)]
4. Matthaios, V.N.; Lawrence, J.; Martins, M.A.G.; Ferguson, S.T.; Wolfson, J.M.; Harrison, R.M.; Koutrakis, P. Quantifying Factors Affecting Contributions of Roadway Exhaust and Non-Exhaust Emissions to Ambient PM_{10-2.5} and PM_{2.5-0.2} Particles. *Sci. Total Environ.* **2022**, *835*, 155368. [[CrossRef](#)] [[PubMed](#)]
5. Thorpe, A.; Harrison, R.M. Sources and Properties of Non-Exhaust Particulate Matter from Road Traffic: A Review. *Sci. Total Environ.* **2008**, *400*, 270–282. [[CrossRef](#)]
6. Bukowiecki, N.; Lienemann, P.; Hill, M.; Furger, M.; Richard, A.; Amato, F.; Prévôt, A.S.H.; Baltensperger, U.; Buchmann, B.; Gehrig, R. PM₁₀ Emission Factors for Non-Exhaust Particles Generated by Road Traffic in an Urban Street Canyon and along a Freeway in Switzerland. *Atmos. Environ.* **2010**, *44*, 2330–2340. [[CrossRef](#)]
7. Grigoratos, T.; Martini, G. Brake Wear Particle Emissions: A Review. *Environ. Sci. Pollut. Res.* **2015**, *22*, 2491–2504. [[CrossRef](#)]
8. Harrison, R.M.; Jones, A.M.; Gietl, J.; Yin, J.; Green, D.C. Estimation of the Contributions of Brake Dust, Tire Wear, and Resuspension to Nonexhaust Traffic Particles Derived from Atmospheric Measurements. *Environ. Sci. Technol.* **2012**, *46*, 6523–6529. [[CrossRef](#)] [[PubMed](#)]
9. Lawrence, S.; Sokhi, R.; Ravindra, K.; Mao, H.; Prain, H.D.; Bull, I.D. Source Apportionment of Traffic Emissions of Particulate Matter Using Tunnel Measurements. *Atmos. Environ.* **2013**, *77*, 548–557. [[CrossRef](#)]
10. Padoan, E.; Amato, F. Vehicle Non-Exhaust Emissions: Impact on Air Quality. In *Non-Exhaust Emissions*; Amato, F., Ed.; Academic Press: Cambridge, MA, USA, 2018.
11. Kumar, P.; Pirjola, L.; Ketzler, M.; Harrison, R.M. Nanoparticle Emissions from 11 Non-Vehicle Exhaust Sources—A Review. *Atmos. Environ.* **2013**, *67*, 252–277. [[CrossRef](#)]
12. Liati, A.; Schreiber, D.; Lugovyy, D.; Gramstat, S.; Dimopoulos Eggenschwiler, P. Airborne Particulate Matter Emissions from Vehicle Brakes in Micro- and Nano-Scales: Morphology and Chemistry by Electron Microscopy. *Atmos. Environ.* **2019**, *212*, 281–289. [[CrossRef](#)]
13. Dimopoulos Eggenschwiler, P.; Schreiber, D.; Papetti, V.; Gramstat, S.; Lugovyy, D. Electron Microscopic Characterization of the Brake Assembly Components (Disc and Pads) from Passenger Vehicles. *Atmosphere* **2022**, *13*, 523. [[CrossRef](#)]
14. Iijima, A.; Sato, K.; Yano, K.; Tago, H.; Kato, M.; Kimura, H.; Furuta, N. Particle Size and Composition Distribution Analysis of Automotive Brake Abrasion Dusts for the Evaluation of Antimony Sources of Airborne Particulate Matter. *Atmos. Environ.* **2007**, *41*, 4908–4919. [[CrossRef](#)]
15. zum Hagen, F.H.F.; Mathissen, M.; Grabiec, T.; Hennicke, T.; Rettig, M.; Grochowicz, J.; Vogt, R.; Benter, T. Study of Brake Wear Particle Emissions: Impact of Braking and Cruising Conditions. *Environ. Sci. Technol.* **2019**, *53*, 5143–5150. [[CrossRef](#)]
16. Dall'Osto, M.; Querol, X.; Amato, F.; Karanasiou, A.; Lucarelli, F.; Nava, S.; Calzolari, G.; Chiari, M. Hourly Elemental Concentrations in PM₂₅ Aerosols Sampled Simultaneously at Urban Background and Road Site during SAPUSS—Diurnal Variations and PMF Receptor Modelling. *Atmos. Chem. Phys.* **2013**, *13*, 4375–4392. [[CrossRef](#)]
17. Gietl, J.K.; Lawrence, R.; Thorpe, A.J.; Harrison, R.M. Identification of Brake Wear Particles and Derivation of a Quantitative Tracer for Brake Dust at a Major Road. *Atmos. Environ.* **2010**, *44*, 141–146. [[CrossRef](#)]
18. Johansson, C.; Norman, M.; Burman, L. Road Traffic Emission Factors for Heavy Metals. *Atmos. Environ.* **2009**, *43*, 4681–4688. [[CrossRef](#)]
19. Sanders, P.G.; Xu, N.; Dalka, T.M.; Maricq, M.M. Airborne Brake Wear Debris: Size Distributions, Composition, and a Comparison of Dynamometer and Vehicle Tests. *Environ. Sci. Technol.* **2003**, *37*, 4060–4069. [[CrossRef](#)] [[PubMed](#)]
20. Hinrichs, R.; Soares, M.R.F.; Lamb, R.G.; Soares, M.R.F.; Vasconcellos, M.A.Z. Phase Characterization of Debris Generated in Brake Pad Coefficient of Friction Tests. *Wear* **2011**, *270*, 515–519. [[CrossRef](#)]
21. Dimopoulos Eggenschwiler, P.; Schreiber, D.; Habersatter, J. Brake Particle PN and PM Emissions of a Hybrid Light Duty Vehicle Measured on the Chassis Dynamometer. *Atmosphere* **2023**, *14*, 784. [[CrossRef](#)]
22. Li, J.; Wang, C.; Chen, X.; Li, A.; Ge, Y.; Wang, Y. Characterization of Brake Wear Particle Emissions from Passenger Cars: A Case Study of Particle Agglomeration and Fragmentation. *J. Environ. Sci.* **2025**, *158*, 790–801. [[CrossRef](#)]
23. Mathissen, M.; Grigoratos, T.; Lahde, T.; Vogt, R. Brake Wear Particle Emissions of a Passenger Car Measured on a Chassis Dynamometer. *Atmosphere* **2019**, *10*, 556. [[CrossRef](#)]
24. Mamakos, A.; Arndt, M.; Hesse, D.; Augsburg, K. Physical Characterization of Brake-Wear Particles in a PM₁₀ Dilution Tunnel. *Atmosphere* **2019**, *10*, 639. [[CrossRef](#)]
25. Iijima, A.; Sato, K.; Yano, K.; Kato, M.; Kozawa, K.; Furuta, N. Emission Factor for Antimony in Brake Abrasion Dusts as One of the Major Atmospheric Antimony Sources. *Environ. Sci. Technol.* **2008**, *42*, 2937–2942. [[CrossRef](#)]
26. Augsburg, K.; Hesse, D.; Feissel, T.; Wenzel, F. Real Driving Emissions Measurement of Brake Dust Particles. In *9th International Munich Chassis Symposium 2018: Chassis.tech Plus*; Springer: Wiesbaden, Germany, 2019; pp. 663–674.
27. Liu, Y.; Chen, H.; Yin, C.; Federici, M.; Perricone, G.; Li, Y.; Margaritis, D.; Shen, Y.; Guo, J.; Wei, T. PM₁₀ Prediction for Brake Wear of Passenger Car during Different Test Driving Cycles. *Chemosphere* **2022**, *305*, 135481. [[CrossRef](#)] [[PubMed](#)]

28. Hagino, H.; Oyama, M.; Sasaki, S. Laboratory Testing of Airborne Brake Wear Particle Emissions Using a Dynamometer System under Urban City Driving Cycles. *Atmos. Environ.* **2016**, *131*, 269–278. [[CrossRef](#)]
29. Alemani, M.; Gialanella, S.; Straffellini, G.; Ciudin, R.; Olofsson, U.; Perricone, G.; Metinoz, I. Dry Sliding of a Low Steel Friction Material against Cast Iron at Different Loads: Characterization of the Friction Layer and Wear Debris. *Wear* **2017**, *376–377*, 1450–1459. [[CrossRef](#)]
30. Mosleh, M.; Blau, P.J.; Dumitrescu, D. Characteristics and Morphology of Wear Particles from Laboratory Testing of Disk Brake Materials. *Wear* **2004**, *256*, 1128–1134. [[CrossRef](#)]
31. Philippe, F.; Xiang, M.; Bressot, C.; Chen, Y.; Guingand, F.; Charles, P.; Loigerot, J.; Morgenev, M. Relevance of Pin-on-Disc and Inertia Dynamometer Bench Experiments for Braking Emission Studies. *J. Phys. Conf. Ser.* **2019**, *1323*, 012025. [[CrossRef](#)]
32. Sinha, A.; Ischia, G.; Menapace, C.; Gialanella, S. Experimental Characterization Protocols for Wear Products from Disc Brake Materials. *Atmosphere* **2020**, *11*, 1102. [[CrossRef](#)]
33. Beji, A.; Deboudt, K.; Khardi, S.; Muresan, B.; Flament, P.; Fourmentin, M.; Lumière, L. Non-Exhaust Particle Emissions under Various Driving Conditions: Implications for Sustainable Mobility. *Transp. Res. Part D Transp. Environ.* **2020**, *81*, 102290. [[CrossRef](#)]
34. Kwak, J.; Kim, H.; Lee, J.; Lee, S. Characterization of Non-Exhaust Coarse and Fine Particles from on-Road Driving and Laboratory Measurements. *Sci. Total Environ.* **2013**, *458–460*, 273–282. [[CrossRef](#)]
35. Grigoratos, T.; Martini, G. Development of a Commonized Methodology for Measuring Brake Wear Particles—Current Status within the PMP IWG. In *8th International Munich Chassis Symposium 2017: Chassis.tech Plus*; Springer: Wiesbaden, Germany, 2017; p. 627.
36. Mathissen, M.; Grochowicz, J.; Schmidt, C.; Vogt, R.; Farwick zum Hagen, F.H.; Grabiec, T.; Steven, H.; Grigoratos, T. A Novel Real-World Braking Cycle for Studying Brake Wear Particle Emissions. *Wear* **2018**, *414–415*, 219–226. [[CrossRef](#)]
37. Grigoratos, T.; Agudelo, C.; Grochowicz, J.; Gramstat, S.; Robere, M.; Perricone, G.; Sin, A.; Paulus, A.; Zessinger, M.; Hortet, A.; et al. Statistical Assessment and Temperature Study from the Interlaboratory Application of the WLTP–Brake Cycle. *Atmosphere* **2020**, *11*, 1309. [[CrossRef](#)]
38. Grigoratos, T.; Mamakos, A.; Arndt, M.; Lugovyy, D.; Anderson, R.; Hafenmayer, C.; Moisio, M.; Vanhanen, J.; Frazee, R.; Agudelo, C.; et al. Characterization of Particle Number Setups for Measuring Brake Particle Emissions and Comparison with Exhaust Setups. *Atmosphere* **2023**, *14*, 103. [[CrossRef](#)]
39. Grigoratos, T.; Mathissen, M.; Vedula, R.; Mamakos, A.; Agudelo, C.; Gramstat, S.; Giechaskiel, B. Interlaboratory Study on Brake Particle Emissions—Part I: Particulate Matter Mass Emissions. *Atmosphere* **2023**, *14*, 498. [[CrossRef](#)]
40. Mathissen, M.; Grigoratos, T.; Gramstat, S.; Mamakos, A.; Vedula, R.; Agudelo, C.; Grochowicz, J.; Giechaskiel, B. Interlaboratory Study on Brake Particle Emissions Part II: Particle Number Emissions. *Atmosphere* **2023**, *14*, 424. [[CrossRef](#)]
41. United Nations. *ECE/TRANS/180/Add.24*; Addendum 24: UN Global Technical Regulation No. 24. UN: New York, NY, USA, 2023.
42. Gramstat, S. Chapter 10—Technological Measures for Brake Wear Emission Reduction: Possible Improvement in Com-Positions and Technological Remediation. In *Non-Exhaust Emissions*; Amato, F., Ed.; Academic Press: Cambridge, MA, USA, 2018; pp. 205–227.
43. Kupper, M.; Schubert, L.; Nachtnebel, M.; Schröttner, H.; Huber, M.P.; Fischer, P.; Bergmann, A. Measurement and Analysis of Brake and Tyre Particle Emissions from Automotive Series Components for High-Load Driving Tests on a Wheel and Suspension Test Bed. *Atmosphere* **2024**, *15*, 430. [[CrossRef](#)]
44. Vishnoi, A.S.; Vansevenant, B.; Beji, A.; Goriaux, M.; Guiot, B.; Azizi, Y.; Messieux, M.; Tassel, P.; Serindat, S.; Quennet, N.; et al. On-Board Characterization of Brake-Wear Emissions from a Heavy-Duty Vehicle in Real-World Driving Conditions. *Atmos. Environ. X* **2025**, *28*, 100379. [[CrossRef](#)]
45. Hagino, H. Brake Wear and Airborne Particle Mass Emissions from Passenger Car Brakes in Dynamometer Experiments Based on the Worldwide Harmonized Light-Duty Vehicle Test Procedure Brake Cycle. *Lubricants* **2024**, *12*, 206. [[CrossRef](#)]

Disclaimer/Publisher’s Note: The statements, opinions and data contained in all publications are solely those of the individual author(s) and contributor(s) and not of MDPI and/or the editor(s). MDPI and/or the editor(s) disclaim responsibility for any injury to people or property resulting from any ideas, methods, instructions or products referred to in the content.